Creep compliance and micromechanics of multi-walled carbon nanotubes based hybrid composites

S. Srikant Patnaik[a], Ashirbad Swain and Tarapada Roy[*]

Department of Mechanical Engineering, National Institute of Technology Rourkela, Rourkela-769008, India

Abstract. This article investigates the properties of nanocomposites (NCs) and carbon fiber reinforced hybrid materials from experimental and numerical studies under different thermal conditions. The multi-walled carbon nanotubes (MWCNTs) are reinforced in the epoxy for the preparation of NCs with the help of ultrasonic probe sonicator. Hand layup technique is used for the preparation of NCs and NCs based carbon fiber reinforced polymer (CFRP) with pre-cured epoxy. To study the dispersion and agglomerations of the reinforcement in matrix phase, the images are captured at high magnification for the MWCNTs, NCs and NCs based CFRP based hybrid material system with the help of transmission electron microscopy (TEM) and environmental scanning electron microscopy (ESEM). At different temperatures, the short term creep and frequency scan tests are performed on the dynamic mechanical analyzer-8000 (DMA-8000) for MWCNTs based NCs, and NCs based CFRP material system respectively. The creep compliance is obtained from DMA-8000. The frequency and temperature dependent material properties of NCs based material system have obtained from the numerical analysis. The Saravanos-Chamis micromechanics (SCM) and strength of material (SOM) methods are implemented to determine the material properties of NCs based CFRP material system. Storage modulus and loss factor are determined in order to study the effect of different MWCNT percentage on the NCs based CFRP material systems. Experimental validation has been done for the suggested NCs based CFRP material system. Responses suggest the damping property is improved by the inclusion of MWCNTs in the matrix phase for CFRP material system. It is further observed that the higher MWCNTs percentage in the matrix phase leads to higher stiffness and damping.

Keywords: MWCNTs; nanocomposite; creep compliance; micromechanics; damping

1. Introduction

After the discovery of CNTs (Ijima 1991), it has fascinated researchers for its remarkable mechanical properties like higher Young's modulus, lower specific weight, high specific surface area for practical applications. Due to its exceptional mechanical and viscoelastic properties it has found scope of applications from aerospace engineering to sports industries. MWCNT's are used as reinforcement has small size of 6 nm and have higher specific volume. A sublayer of nano-film (Chandra *et al.* 1999, Koratkar *et al.* 2002) in a piezo-silica composite beam can enhance 200% damping performance and 30% bending stiffness without affecting the weight of structure. The presented studies (Zhau *et al.* 2004. Koratkar *et al.* 2005) suggests that addition of 2% CNT in matrix

---

*Corresponding author, Assistant Professor, E-mail: tarapada@nitrkl.ac.in
[a]Ph.D. Student, E-mail: shree1043@gmail.com

phase can lead to 1000% increase of the loss modulus of a bar under axial cyclic loading. Experiments conducted (Rajoria *et al.* 2005) on single and multi-walled CNTs based nanocomposite observed that enhancement in damping ratio is more dominant than that of stiffness. A mathematical model presented (Lin *et al.* 2010) to obtain energy dissipation between the nanotubes and the resin based on the interfacial friction. Vibration damping characteristics of MWCNT based hybrid composite, the presented studies (Khan *et al.* 2011) found that the damping ratio of the hybrid composites is increased with the addition of CNTs. The thermal and mechanical properties of MWCNT reinforced epoxy based material are reported (Theodore *et al.* 2011, Gojny *et al.* 2004) which indicated that improved dispersion can be achieved by chemical functionalization of inclusions in the matrix phase. The material properties of CNT based materials with tensile and dynamic mechanical analyser have been determined (Montazeri and Montazeri 2011). Author (Thostenson and Chou 2006) suggested that for mixing of CNTs into polymer, high shear stress must be employed to get better dispersion. The review article reported (Ma *et al.* 2010) the different dispersion and functionalization methods of carbon nanotubes in the matrix phase. Authors concluded that the ultra-sonication and chemical functionalization techniques give better dispersion of CNT in matrix phase. The experimental procedure (Hirsch 2002) suggested the essential steps based on the interaction between CNT polymer from chemical functionalization and physical methods. Author Balasubramanian and Burghard (2005) summarized the advantages and disadvantages of chemically functionalization process for CNTs into matrix phase. The study carried out on different experimental procedures (Zhang *et al.* 2015, Rahmanian *et al.* 2014) for the preparation of the high hybrid composites containing short fibers with chemical vapour deposition method. Jia *et al.* (2011) presented that the inclusion of CNTs in nanocomposites, decrease in creep strains by 53% compared to epoxy matrix. The long term creep behaviour of the nanocomposites by time temperature superposition in dynamic mechanical analyser was also predicted. Indentation experiments were carried out (Tehrani *et al.* 2011) at high temperature to determine the mechanical properties of nanocomposite based material system. The reported article (Dul *et al.* 2018) proposed the combination of acrylonitrile-butadiene-styrene (ABS) filaments with graphene at 4 weight percentage for higher elasticity and storage modulus. Author (Yao *et al.* 2013) studied the mechanical properties of nanocomposites which were prepared by in-situ polymerization method. Creep and time temperature superposition tests were conducted to obtain the viscoelastic properties of nanocomposites. Investigation have been carried out to obtain (Boris *et al.* 2018) the viscoelastic properties of short fibers reinforced composite with dynamic mechanical analyser. Author (Knapp *et al.* 2015) characterized the damping behaviour of the thin film passive layer of the composite which has size of less than 50 μm thickness. The investigation has been done by Chandra *et al.* (2002) for the damping coefficients of fiber reinforced composites based on micromechanical method to observe the effects of the shape and volume fractions of the reinforcement in the composite materials. The viscoelastic material modelling (Swain and Roy 2017) of hybrid composite material has been carried out based on the Mori-Tanaka micromechanics. The elastic properties (Swain *et al.* 2016, Swain *et al.* 2016) of carbon fiber reinforced hybrid composite material using Mori-Tanaka and strength of material methods are evaluated. Comparative studies have been presented (Treviso *et al.* 2015) by reviewing the different methods of damping properties analysis in composite materials for different models. MWCNTs have also shown to be having superior static and dynamic characteristics when subject to different loads (Ghayesh *et al.*). The effect of MWCNTs on the viscoelastic properties and dynamics of the structures has also been studied (Ghayesh *et al.*).

From the literatures, it is cleared that in many areas, improved damping of the NC based material system is required. For different applications, carbon-fiber reinforced NC based material system will

be very useful. Such materials possess good load carrying capacity and are subjected to dynamic loads in real life operations that cause vibrations. Hence, the study concerning damping problems of such material system is of practical significance and great importance. Research in this area has already been started but lack of fabrication techniques and experimental studies are yet to be explored for better practical application of materials made by CNTs.

The present study addresses the experimental and numerical techniques for the determination of the viscoelastic properties (such as storage and loss moduli) of nanocomposites based hybrid materials under different hygrothermal conditions based on creep compliances. The MWCNT's are used as reinforcement has small size of 6 nm and higher specific volume. MWCNTs are mixed in 0%, 4% and 8% by volume in the pre-cured epoxy to prepare samples from the sonication dispersion. The samples are prepared with sharp edges and required dimensional accuracy. For the agglomeration studies in the sample, images are captured with the help of environmental scanning electron microscopy (ESEM). The random orientation of MWCNT in polymer and uniform size of MWCNT are considered in this study. The samples are experimented on DMA-8000 for short term creep test and creep compliance is obtained. With creep compliance further numerical study is carried out to determine the stress relaxation, storage and loss modulus. Material properties and damping characteristics of NC and HC are also obtained by the numerical study.

2. Experimental

2.1 Mixing of MWCNT in polymer

The epoxy is reinforced by MWCNTs with the help of ultrasonic probe sonicator. Mixing is done for 3 hours to disperse the inclusions in the matrix phase. Epoxy is Pre-cured at 45°C for 30 minutes before mixing, and then MWCNTs are reinforced in the epoxy. The MWCNTs are mixed 4% and 8% respectively by volume in epoxy.

2.2 Drying and sample preparation

The bottom surface of the mould is preheated to 45°C and after applying the mould relieving spray onto the whole mould surface, the dispersed MWCNTs reinforced epoxy is poured into the mould for the NC material based samples. For hybrid composite (HC) samples, CNT reinforced polymer brushed onto the fibers which are placed unidirectional (UD) in the mould. NC material based sample and hybrid composite samples are prepared with hand layup technique. Then it is allowed to dry for minimum of 72 hours. The samples are extracted from the mould with the required dimensional accuracy.

2.3 Creep and frequency scan test on DMA-8000

Short term creep test is conducted on DMA-8000 for the different NC samples to obtain creep compliance. Creep test is done for different volume fractions i.e., 0%, 4% and 8%, of the MWCNT in the epoxy at different temperatures i.e., 0°C, 25°C and 50°C respectively. NC sample is fixed under tension support as shown in Fig. 1. Frequency scan tests are also carried out on DMA-8000 to obtain the storage modulus and loss factor for the hybrid material system. The sequential procedure is shown in Fig. 2. The NC samples made as per the ASTM standards are shown in Fig. 3.
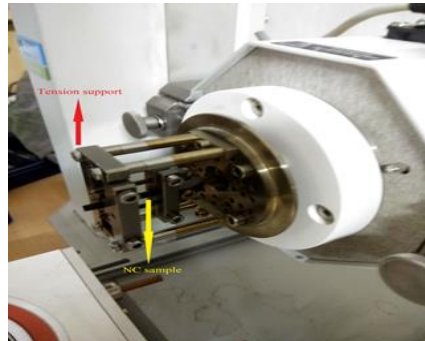
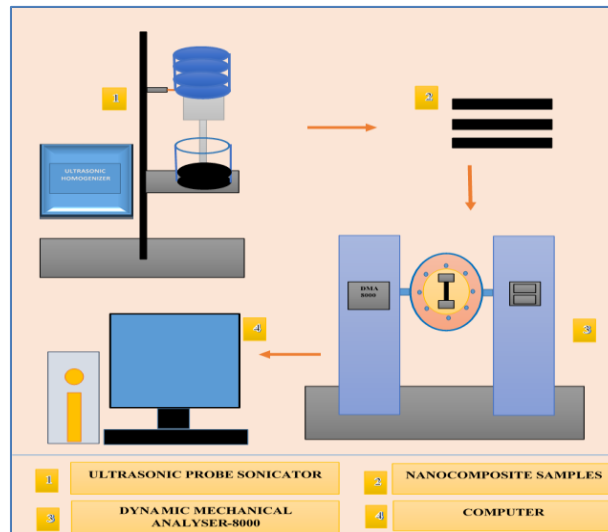Fig. 1 DMA-8000 image with NC sample under tension support

Fig. 2 Schematic diagram of Experimental procedure

3. Experimental and mathematical modelling for NC and HC material system

Material property of the NC based material systems is obtained experimentally with DMA-8000. The present mathematical modelling cosists of Saravanos-Chamis micromechanics (SCM) and strength of material (SOM). Analysis of NC and hybrid composite is presented in the subsections.

3.1 Experimental and numerical modelling for NC

NC based samples are prepared with mixing the MWCNT in the pre-cured polymer matrix. The MWCNT is mixed with volume fraction of 0%, 4% and 8% seperately. The polymer matrix nanocomposite (PMNC) exhibits higher material property with higher volume percentage of MWCNT. The NC based samples are prepared with the required dimensional accuracy as per ASTM standard and creep test is conducted on DMA-8000.

For such material based samples, creep compliance is obtained with different volume fractions at different temperatures. Further numerical analysis is carried out with laplace transform to obtain
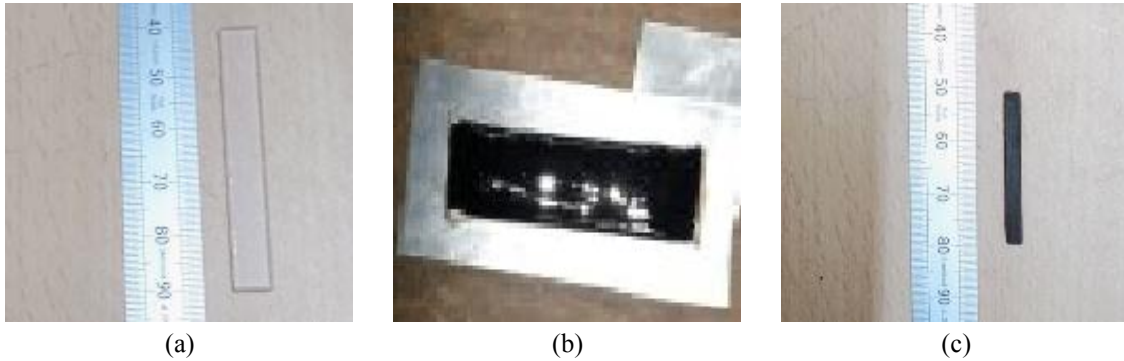
(a)   (b)   (c)

Fig. 3 Images of different samples of (a) polymer, (b) nancomposite and (c) hybrid composite
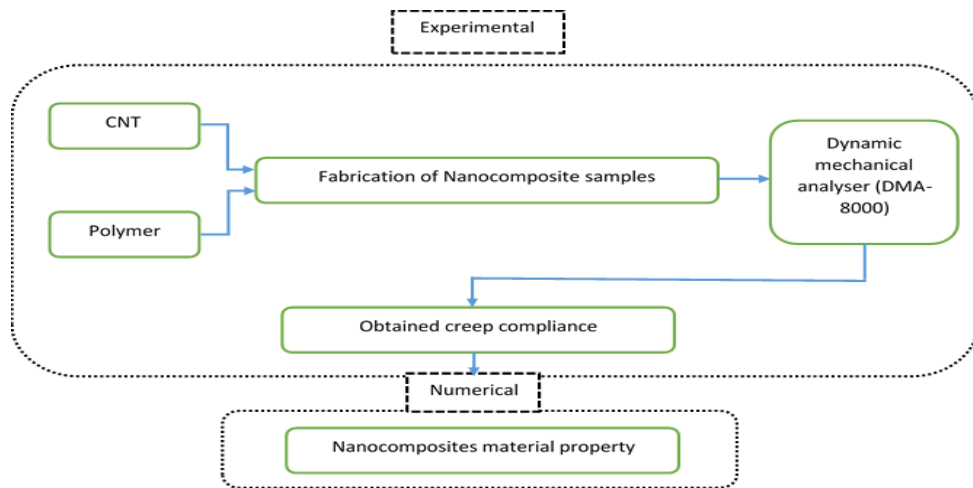

Fig. 4 Experimental and numerical constituents of CNTs-based NC

the storage modulus and loss modulus for NC based material.

$$E(\omega) = E_0 + \frac{E(i)\omega^2}{\omega^2 + \frac{1}{\tau(i)^2}}$$

(1)

Where, $E(\omega)$, E_0, ω are frequency dependent modulus, instenteneous modulus and frequency respectively. $\tau(i)$, and $E(i)$ are prony constants. Succession 1 shows in the Fig. 4 for NC based material system.

3.2 Experimental and numerical modelling for HC

Carbon fiber reinforced PMNC hybrid composite samples are fabricated in different volume fractions (i.e., 6%, 15.3%, 32.5% and 49.8%) with required dimensions. The frequency scan test is conducted on DMA-8000 and frequency dependent material properties are obtained. Numerical investigation is carried out for long fibers reinforced PMNC from Saravanos-Chamis micromechanics and strength of material methods. The material properties obtained numerically are
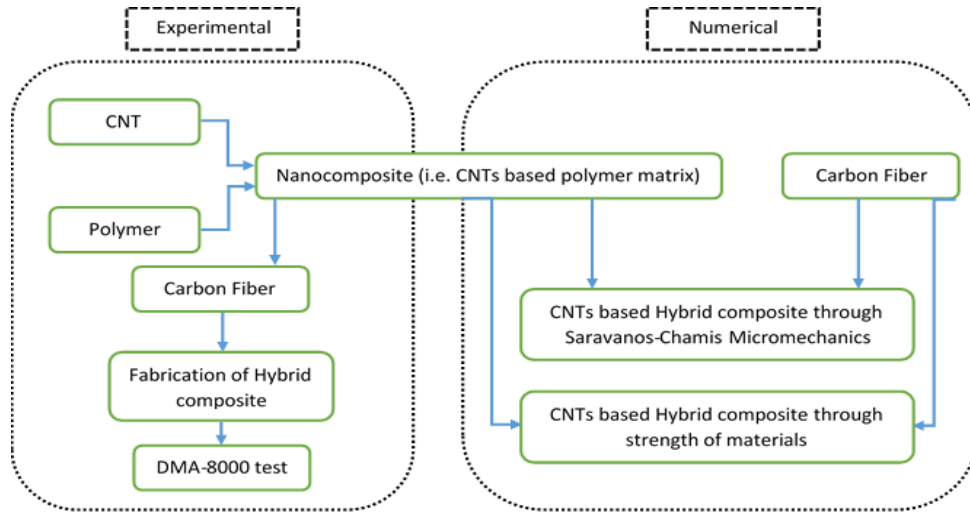
Fig. 5 Experimental and numerical constituents of CNTs-based carbon fiber reinforced HC

compared with the experimental reults. Succession 2 shows in the Fig. 5 for HC based material system.

4. Mathematical formulation

4.1 Mathematical formulation for fiber reinforcement from Saravanos-Chamis micromechanics (Chandra et al. 2002)

Saravanos and Chamis micromechanics (SCM) methods considered the fiber representative volume element (RVE) of square packing array as shown in figure 6. SCM proposed a mathematical model of the properties of hybrid composite consisting of reinforcement and matrix phase. The stresses and stains are considered uniform throughout the hybrid composite from rule of mixture.

The longitudnal and transverse modulus of hybrid composite can be expressed as

$$E_{11} = E_{f11} V_f + E_m V_m \tag{2}$$

$$E_{22} = \left(1 - \sqrt{V_f}\right) E_m + \frac{\sqrt{V_f} E_m}{1 - \sqrt{V_m \left(1 - \dfrac{E_m}{E_{f22}}\right)}} \tag{3}$$

Further, in-plane shear modulus and transverse shear modulus are given by

$$G_{12} = \left(1 - \sqrt{V_f}\right) G_m + \frac{\sqrt{V_f} G_m}{1 - \sqrt{V_f} \left(1 - \dfrac{G_m}{G_{f12}}\right)} \tag{4}$$
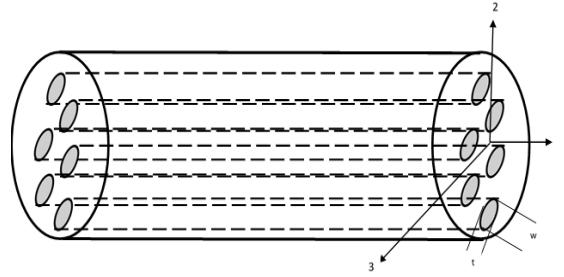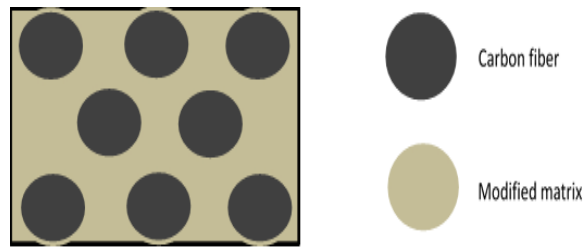
Fig. 6 Square packing array of reinforced fibers

Fig. 7 Hexagonal packing of reinforced fibers

$$G_{23} = \frac{E_{22}}{2(1 + v_{23})} \tag{5}$$

Further, in-plane shear damping and transverse shear damping are given by

$$\eta_{12} = \eta_{f12} \sqrt{V_f} \frac{G_{12}}{G_{f12}} + \eta_m \left(1 - \sqrt{V_f}\right) \frac{G_{12}}{G_m} \tag{6}$$

$$\eta_{23} = \eta_{f23} \sqrt{V_f} \frac{G_{23}}{G_{f23}} + \eta_m \left(1 - \sqrt{V_f}\right) \frac{G_{23}}{G_m} \tag{7}$$

4.2 Mathematical formulation for fiber reinforcement from strength of materials (Swain et al. 2016, Swain et al. 2016)

Fig. 7 shows hexagonal representative volume element (RVE) of hybrid composite consisting PMNC reinforced by carbon fiber. The strains in the modified matrix (NC), carbon fiber and hybrid composite are equal in fiber direction and the stresses are equal in the transverse direction from isofield conditions. Perfect bonding is considered between reinforcemen (carbon fiber) and modified matrix. The constitutive relations for the hybrid composite are written below

$$\{\sigma^r\} = [C^r]\{\varepsilon^r\}; r = f, NC. \tag{8}$$

$$E_{PMNC} = \frac{9K_{PMNC} G_{PMNC}}{3K_{PMNC} + G_{PMNC}} \tag{9}$$

<center>(a)   (b)   (c)</center>
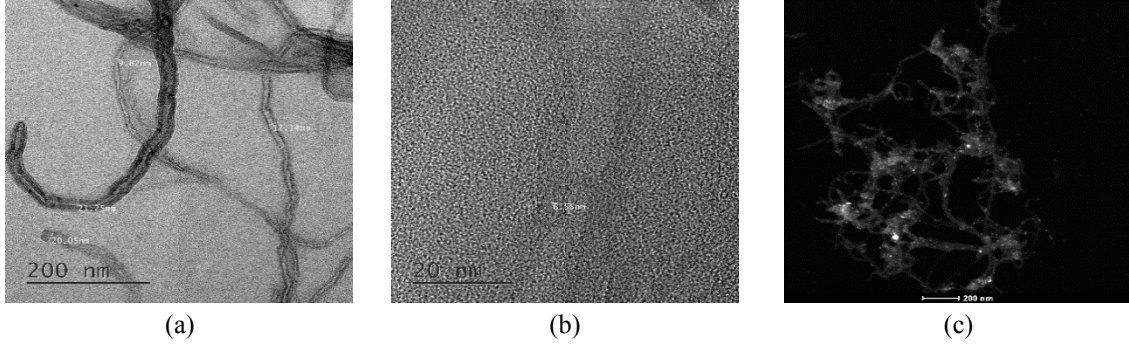
Fig. 8 (a) Bright field, (b) HRTEM and (c) HAADF TEM images of MWCNT at Nano-meter scale

From rule of mixture, the volume fraction of fiber reinforcement and NC based modified matrix in HC is

$$v_f + v_{NC} = 1 \tag{10}$$

The strains and stresses in the hybrid composite in longitudinal and transverse direction considered from iso-field conditions and rule of mixture are written as

$$\begin{aligned}
&\{\varepsilon_1^f \quad \sigma_2^f \quad \sigma_3^f \quad \sigma_{23}^f \quad \sigma_{13}^f \quad \sigma_{12}^f\}^T \\
&= \{\varepsilon_1^{NC} \quad \sigma_2^{NC} \quad \sigma_3^{NC} \quad \sigma_{23}^{NC} \quad \sigma_{13}^{NC} \quad \sigma_{12}^{NC}\}^T \\
&= \{\varepsilon_1^{HC} \quad \sigma_2^{HC} \quad \sigma_3^{HC} \quad \sigma_{23}^{HC} \quad \sigma_{13}^{HC} \quad \sigma_{12}^{HC}\}^T,
\end{aligned} \tag{11}$$

$$\begin{aligned}
&v_f\{\sigma_1^f \quad \varepsilon_2^f \quad \varepsilon_3^f \quad \varepsilon_{23}^f \quad \varepsilon_{13}^f \quad \varepsilon_{12}^f\}^T \\
&+ v_{NC}\{\sigma_1^{NC} \quad \varepsilon_2^{NC} \quad \varepsilon_3^{NC} \quad \varepsilon_{23}^{NC} \quad \varepsilon_{13}^{NC} \quad \varepsilon_{12}^{NC}\}^T \\
&= \{\sigma_1^{HC} \quad \varepsilon_2^{HC} \quad \varepsilon_3^{HC} \quad \varepsilon_{23}^{HC} \quad \varepsilon_{13}^{HC} \quad \varepsilon_{12}^{HC}\}^T.
\end{aligned} \tag{12}$$

The expression of stress and strain for HC lamina is obtained from above equations and can be written as

$$\{\sigma^{HC}\} = [C^{HC}]\{\varepsilon^{HC}\}, \tag{13}$$

Where,
$$[C^{HC}] = [C_1][V_3]^{-1} + [C_2][V_4]^{-1}. \tag{14}$$

Other terms in above equation are mentioned in the appendix.

5. Results and discussion

5.1 Based on TEM and ESEM test for NC and HC

MWCNTs are treated in sonication bath for 30-45 minutes, and then with the help of carbon grid, 2-dimensional images are captured on nanoscale. Fig. 8 (a) & (b) shows the bright field and
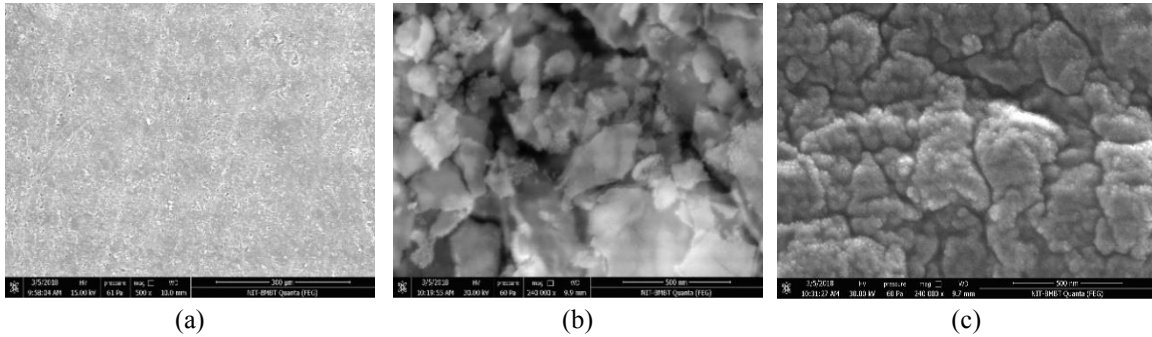
(a)   (b)   (c)

Fig. 9 ESEM images of NC samples containing (a) 0%, (b) 4% and (c) 8% of MWCNT
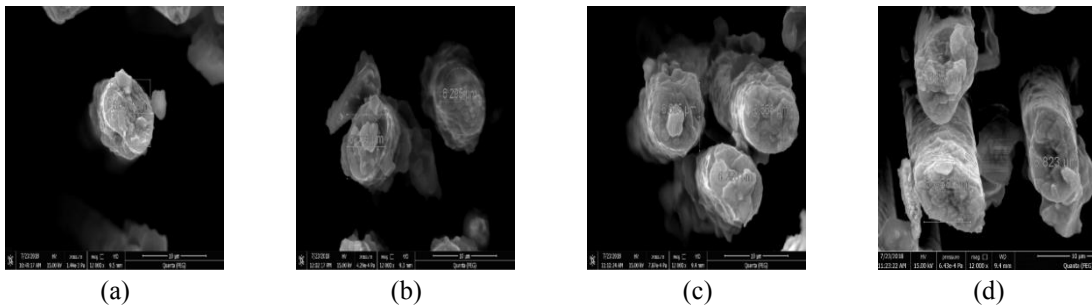

(a)   (b)   (c)   (d)

Fig. 10 ESEM images of HC samples containing with (a) 6%, (b) 15.3%, (c) 32.5% and (d) 49.8% of carbon fiber

high resolution transmission electron microscopy (HRTEM) image of the MWCNT to estimate the overall distribution on the carbon coated copper grid at a lower magnification. Bright field image depicts the dimension of the MWCNTs sample where the average thickness of the Nanotubes ranges from 6 to 10 nm. Fig. 8(c) shows the high angle annular dark field (HAADF) detector image which estimated and confirmed the presence and distribution of MWCNTs in the grid. Scanning transmission electron microscopy (STEM) imaging and analysis is carried out to obtain the sample (MWCNTs) images by diffracted electron beam.

Fig. 9 shows the ESEM images of NCs at high magnification consisting of 0%, 4% and 8% volume fraction inclusion of MWCNT respectively. The agglomeration can be clearly seen in the images by the increasing volume fraction of the MWCNT in the epoxy. Whereas Fig. 10 shows the ESEM images of HC at high magnification consisting the carbon fiber of 6%, 15.3%, 32.5% and 49.8% volume fraction respectively.

5.2 Based on creep test on DMA-8000

Creep compliance is obtained for NC materials with 0%, 4% and 8% volume fraction of MWCNT from DMA-8000 at different thermal conditions, i.e., 0°C, 25°C and 50°C respectively. Short term creep test is conducted on DMA which are shown in Fig. 11(a), 12(a) and 13(a) for different temperatures respectively.

Further creep compliance is predicted through power law curve fitting in time domain as shown in Fig. 11(b), 12(b) and 13(b) for different temperatures respectively. Fig. 14(a), 15(a) and 16(a)
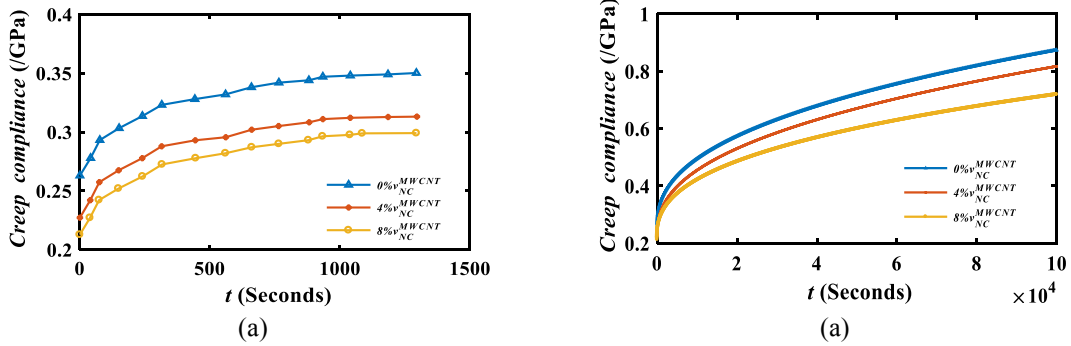
Fig. 11 Variation of (a) short term and (b) long term creep compliance of NC samples at 0°C
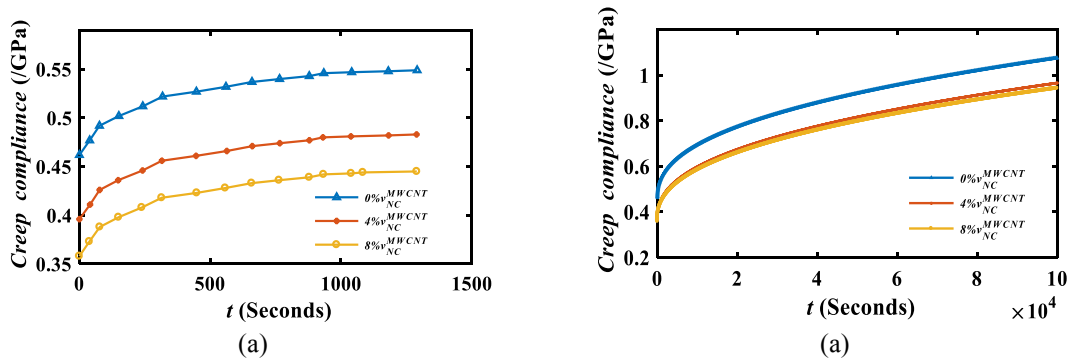

Fig. 12 Variation of (a) short term and (b) long term creep compliance of NC samples at 25°C
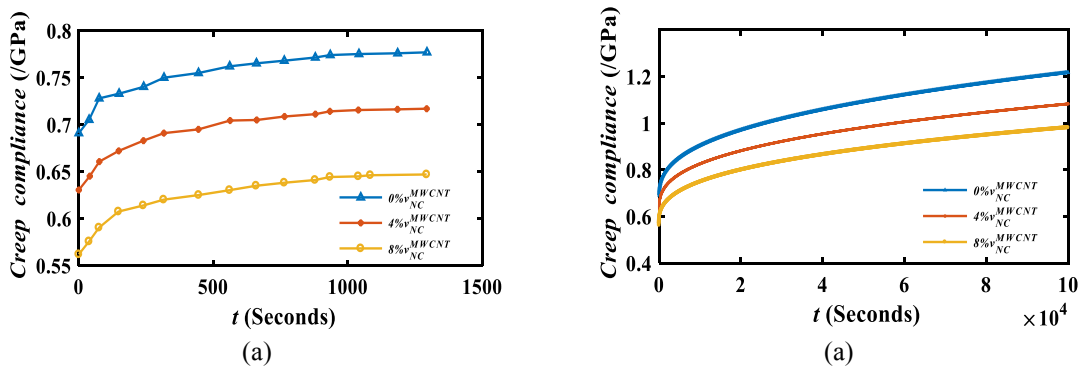

Fig. 13 Variation of (a) short term and (b) long term creep compliance of NC samples at 50°C

shows the creep compliance for the same volume fraction of MWCNT in different temperatures i.e., 0°C, 25°C and 50°C respectively. Through power law curve fitting, further prediction of creep compliance in time domain is shown in 14(b), 15(b) and 16(b).

5.3 Based on numerical prediction of NCs viscoelastic properties

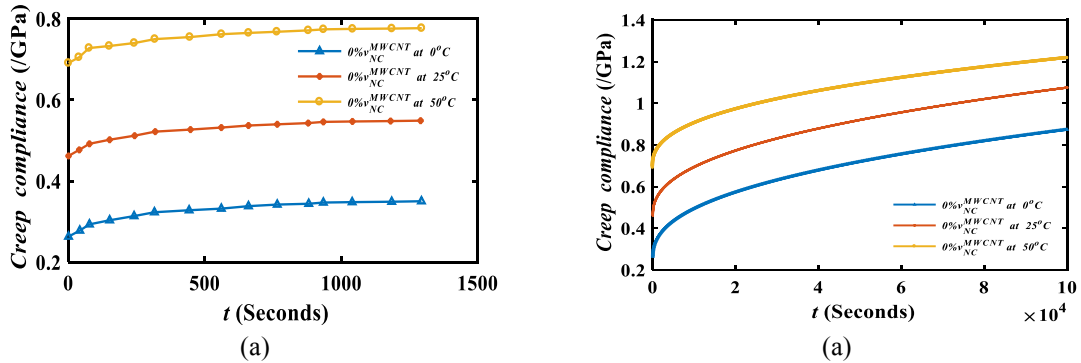Creep compliance is obtained for different NC based materials from DMA-8000 and Prony series

Fig. 14 Variation of (a) short term and (b) long term creep compliance of NC samples containing 0% of MWCNT
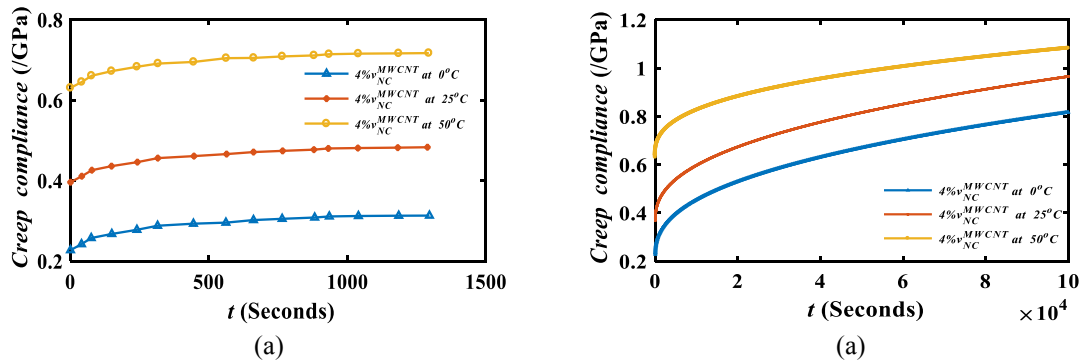

Fig. 15 Variation of (a) short term and (b) long term creep compliance of NC samples containing 4% of MWCNT
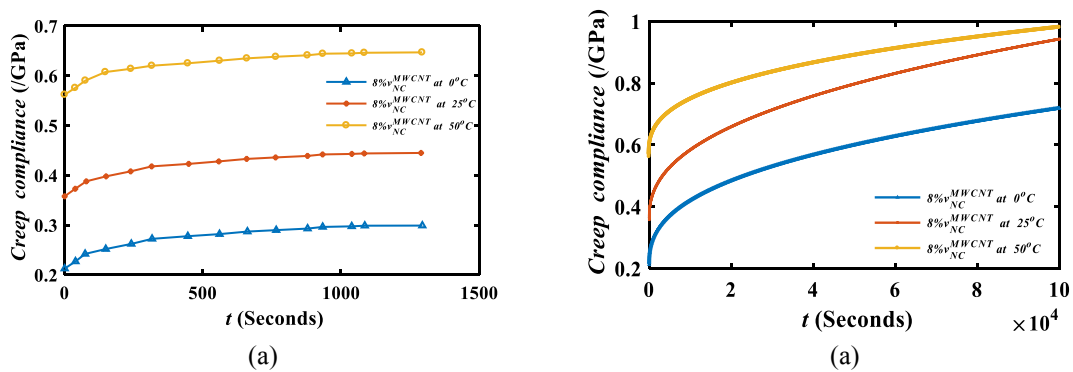

Fig. 16 Variation of (a) short term and (b) long term creep compliance of NC samples containing 8% of MWCNT

is used to obtain the relaxation modulus in time domain which is shown in Fig. 17 at different temperatures. Significant effect of MWCNT is observed on relaxation modulus which increases at lower temperatures. The Laplace transform is used to convert the relaxation modulus from time

Table 1 Validation of NC material properties with increasing volume fraction of MWCNT (Montazeri and Montazeri 2011)

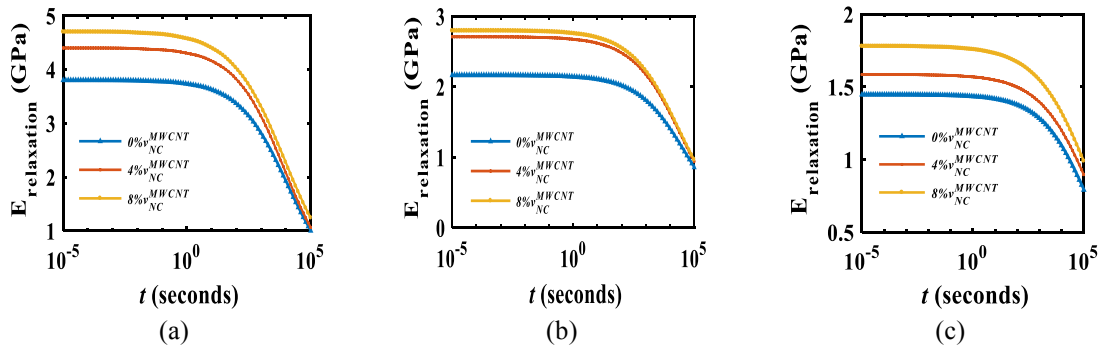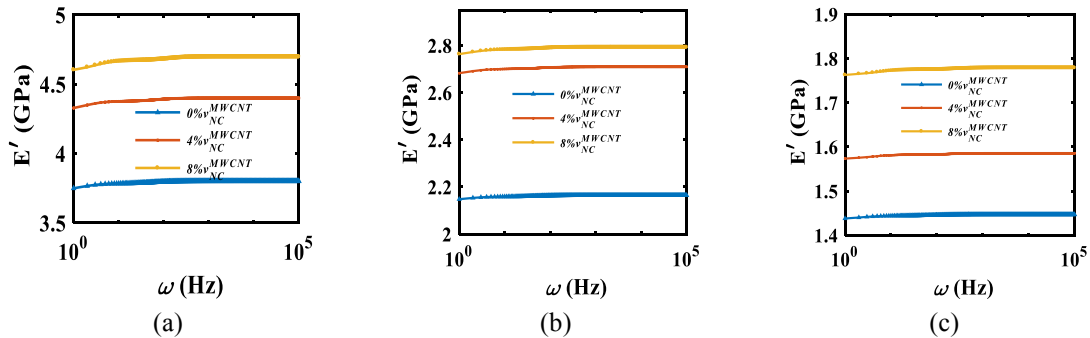| Constituents of NC	Reference [30] (GPa)	% increase (×100)	Present (GPa)	% increase (×100)
Epoxy	3.43	0	2.15	0
4% volume of MWCNT	3.951	0.1518	2.69	0.2511
8% volume of MWCNT	4.225	0.2317	2.77	0.2883

Fig. 17 Variation of relaxation modulus with different volume fraction of MWCNT at (a) 0°C, (b) 25°C and (c) 50°C

Fig. 18 Variation of E' with different volume fraction of MWCNT at (a) 0ºC, (b) 25ºC and (c) 50ºC

domain to frequency domain and the storage modulus and loss factor for such NC based materials are obtained which are shown in Figs. 18 and 19.

The storage modulus of said materials increases and the loss factor decreases by the inclusion of MWCNT in the matrix phase. The MWNCT improved the Young's modulus of polymer significantly which is validated from Montazeri and Montazeri (2011) shown in Table 1.

5.4 Based on Saravanos-Chamis micromechanics (SCM) and strength of materials (SOM) for HC

SCM and SOM mathematical models are used for long fiber reinforcement in the matrix phase. SCM and SOM models employ the square and hexagonal packing array RVE of the fiber in the matrix phase.
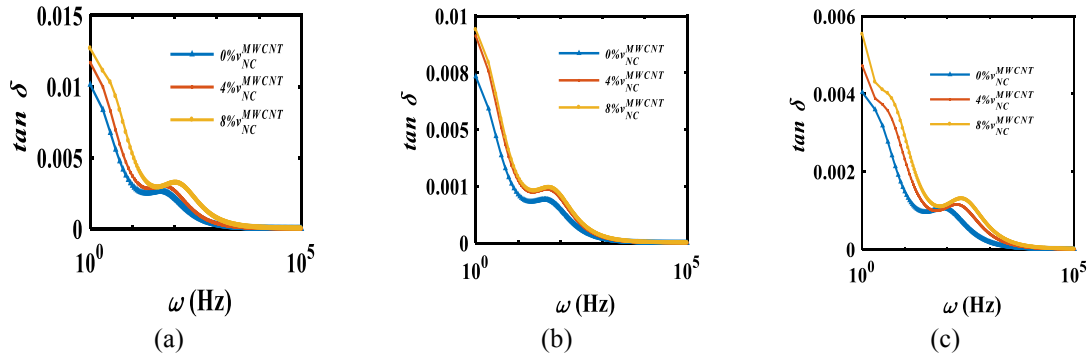
Fig. 19 Variation of E' with different volume fraction of MWCNT at (a) 0ºC, (b) 25ºC and (c) 50ºC
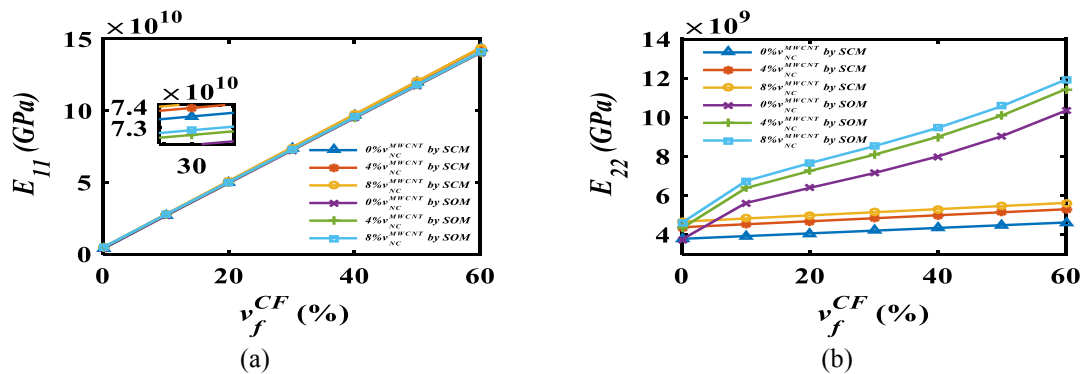

Fig. 20 Variation of (a) E_{11} and (b) E_{22} with the volume fraction of the reinforcement at 0°C

Table 2 Basic properties of CFRP Based HC Constituents

Properties	Carbon fiber	MWCNT	Epoxy
E (GPa)	236.4	800	2.15
Poisson ratio	0.22	0.3	0.34
Density (kg/m^3)	1800	2400	1150

MATLAB codes are used to depict the material properties of CFRP hybrid composite material at different temperatures i.e., 0°C, 25°C and 50°C. Longitudinal and transverse modulus of the CFRP based hybrid material system, increases with the increase in volume fraction of the reinforcement. Significant effect of the MWCNT is observed on the shear modulus and shear loss factor of such CFRP material system. Figs. 20-28 shows the variation in the material properties of such material system at different temperatures. It is apparent that at any volume fraction of the carbon fiber, the MWCNT in the RVE increases the elastic and damping properties. Longitudinal and transverse modulus increases with the increase of volume fraction of carbon fiber, whereas the loss factor and shear loss factor decreases significantly. The materials i.e., MWCNT, carbon fiber and epoxy, which are used to prepare NCs and HCs are procured from ADNANO technologies and HINDOOSTAN composites. The material properties of the constituents of CFRP based material system are mentioned in the Table 2.
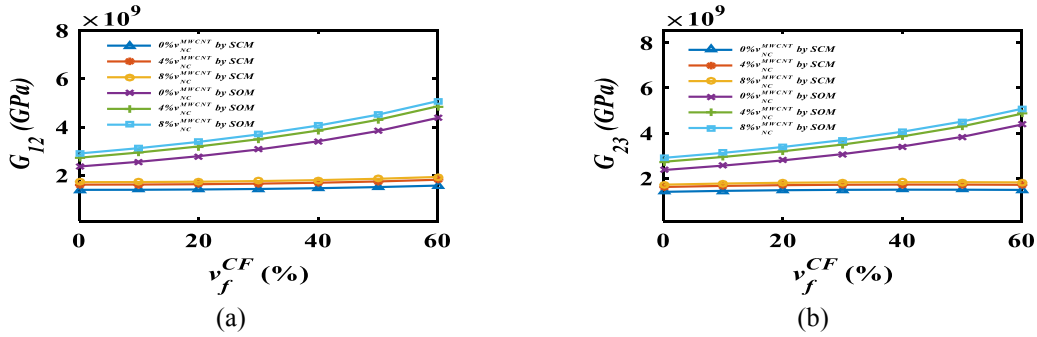
Fig. 21 Variation of (a) G_{12} and (b) G_{23} with the volume fraction of the reinforcement at 0°C
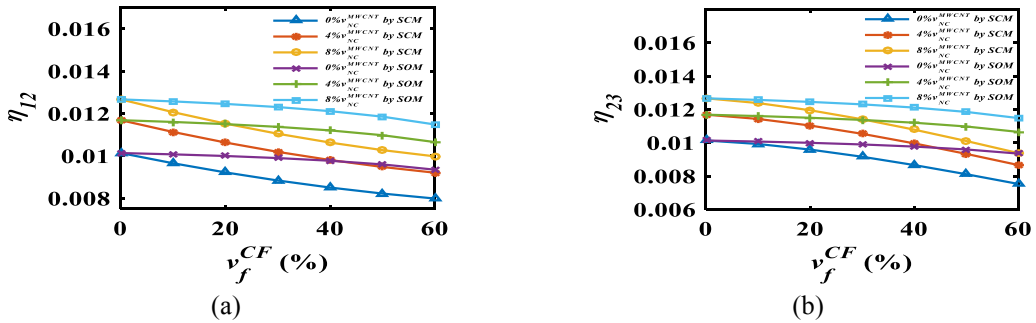

Fig. 22 Variation of (a) η_{12} and (b) η_{23} with the volume fraction of the reinforcement at 0°C

Fig. 23 Variation of (a) E_{11} and (b) E_{22} with the volume fraction of the reinforcement at 25°C

Fig. 24 Variation of (a) G_{12} and (b) G_{23} with the volume fraction of the reinforcement at 25°C

Fig. 25 Variation of (a) η_{12} and (b) η_{23} with the volume fraction of the reinforcement at 25°C
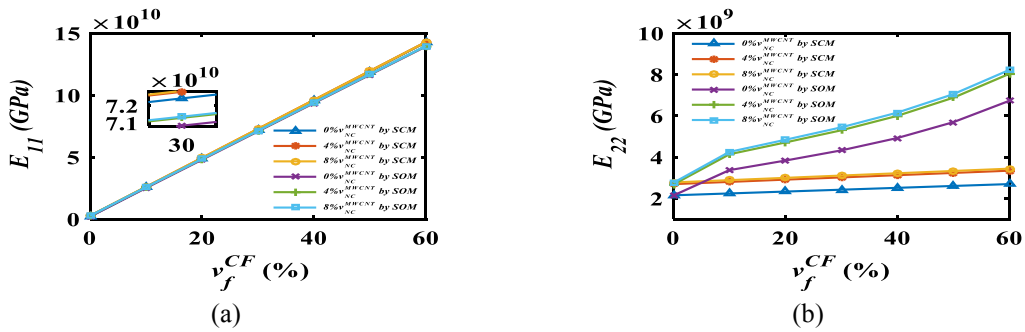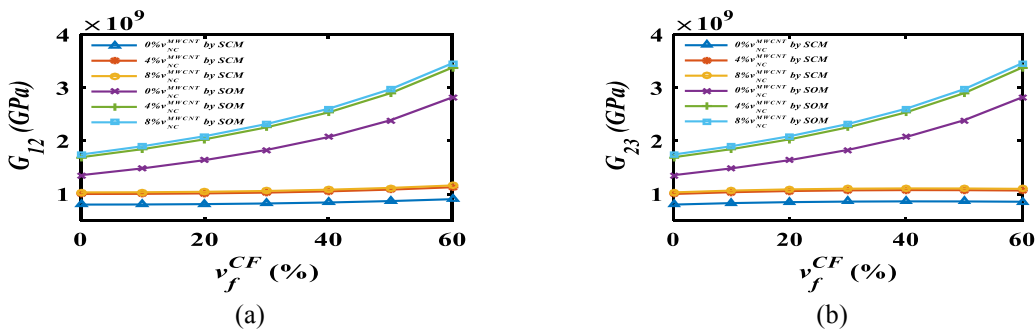

Fig. 26 Variation of (a) E_{11} and (b) E_{22} with the volume fraction of the reinforcement at 50°C
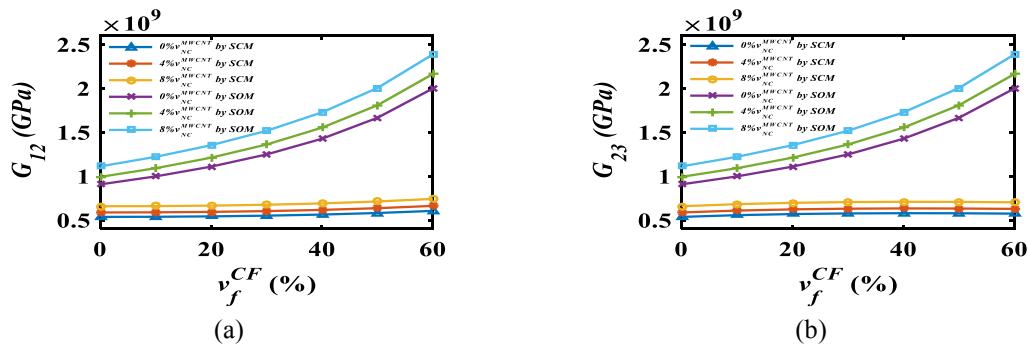
Fig. 27 Variation of (a) G_{12} and (b) G_{23} with the volume fraction of the reinforcement at 50°C

5.5 Based on experimental comparison of PMNC based HC

CFRP based hybrid composite samples are fabricated with 6%, 15.3%, 32.5% and 49.8% volume fraction. Frequency scan test is conducted for such CFRP samples on DMA-8000 to obtain the longitudinal modulus (E_{11}), transverse modulus (E_{22}) and loss factors (tanδ) at 25°C. These results are plotted with numerical results which were obtained from SCM and SOM methods. Experimental comparison has been carried out for the properties of CFRP based hybrid material system. It is observed that the involvement of MWCNT increases the damping properties significantly at
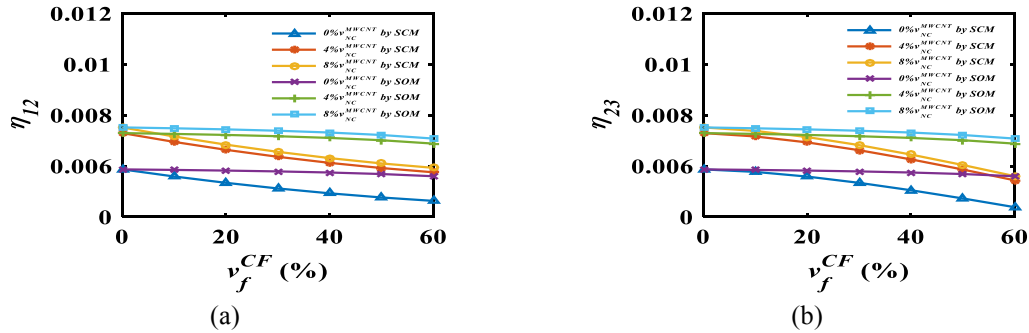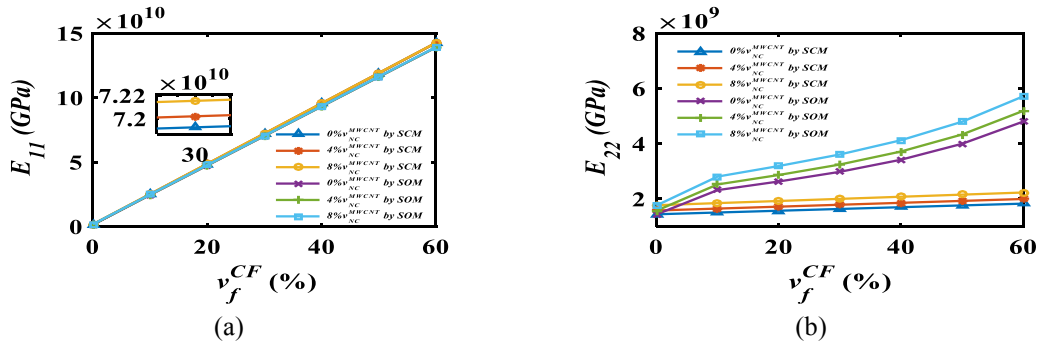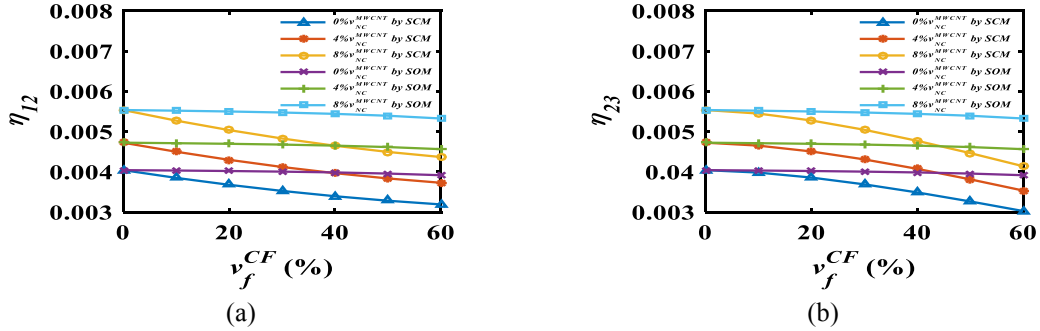
Fig. 28 Variation of (a) η_{12} and (b) η_{23} with the volume fraction of the reinforcement at 50°C
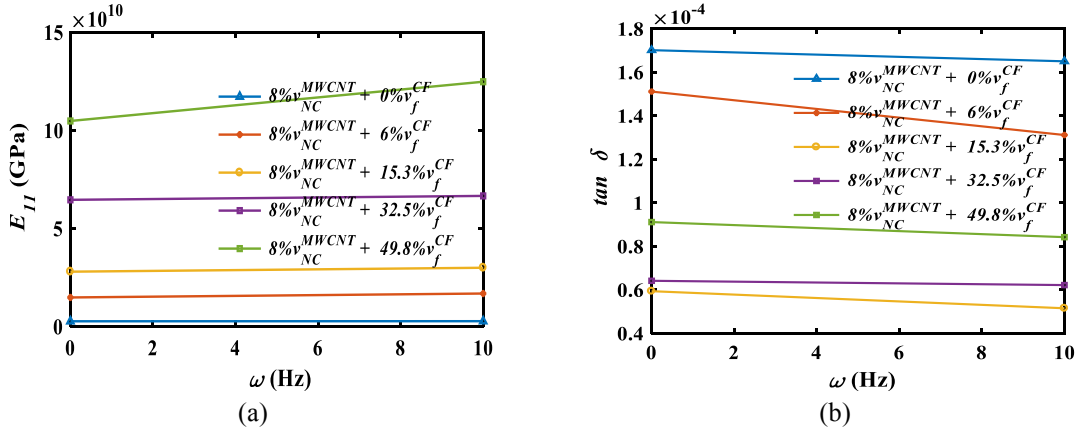
Fig. 29 Variation of (a) E_{11} and (b) longitudinal loss factor in frequency domain at 25°C
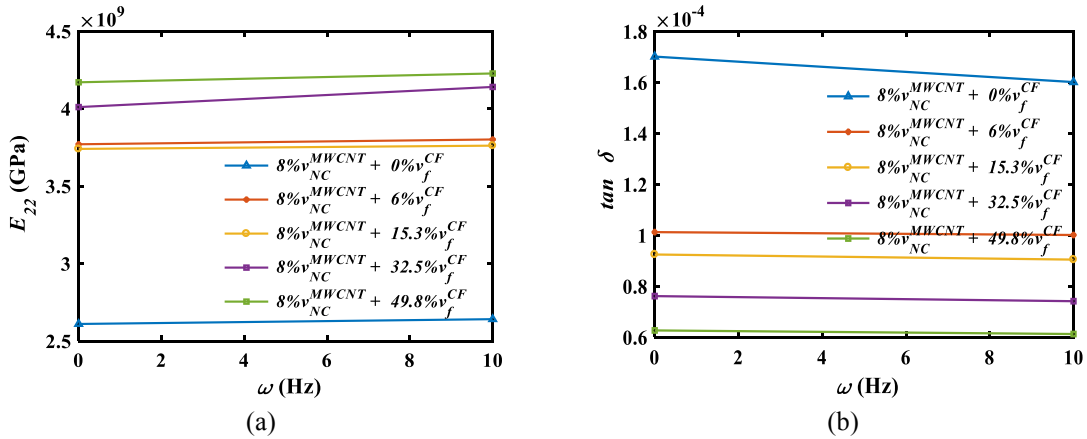
Fig. 30 Variation of (a) E_{22} and (b) transverse loss factor in frequency domain at 25°C

different volume fraction of carbon fiber as shown in Table 3.

Experiments are performed on DMA-8000 at different frequencies to obtain the material properties of such CFRP hybrid material system. Experimental material properties of such CFRP

Table 3 Comparison of experimental and numerical results of HC material properties at 25°C

| Method	CF (%)	E_{11} (GPa)	ζ_{11} (×10^{-4})	E_{22} (GPa)	ζ_{22} (×10^{-4})
Experimental	0	2.731	1.7	2.731	1.7
SCM	6.0	16.96	3.1	2.85	2.1
SOM	6.0	17.04	3.2	3.5	3.1
Experimental	6.0	14.755	1.5	3.77	1.1
SCM	15.3	38.95	1.3	2.91	1.4
SOM	15.3	38.3	1.4	3.83	2.0
Experimental	15.3	27.89	5.9	3.84	9.01
SCM	32.5	79.97	9.1	3.74	1.2
SOM	32.5	78.8	9.3	4.12	1.5
Experimental	32.5	64.51	6.4	4.11	7.6
SCM	49.8	121.27	2.1	3.61	1.0
SOM	49.8	119.43	3.0	4.35	1.1
Experimental	49.8	104.7	9.1	4.57	6.2

based material system for different volume fraction of carbon fiber are shown in Figs. 29 and 30 at 25°C. As the frequency increases, the longitudinal and transverse material properties increase significantly. The comparison of experimental results and numerical results are shown in Table 3. It is evident from the Table 3, that experimental result shows, good damping properties of CFRP based hybrid material system and the effect of the agglomeration on the longitudinal and transverse modulus.

6. Conclusions

Present study proposes the combination of experimental and numerical methodology for determination of viscoelastic properties of NC based hybrid materials based on creep test using dynamic mechanical analysis under different thermal environment. NC and CFRP based hybrid composite materials are fabricated from ultrasonic probe sonicator and hand layup technique. MWCNTs are used as inclusion and carbon fiber as reinforcement. TEM and ESEM are used to capture the high magnification images for agglomeration study and it is observed that higher the MWCNTs in the polymer, higher is the agglomeration. Creep compliance is obtained for NC from DMA-8000 under different thermal conditions. Prony series is used to determine the time dependent relaxation modulus and further laplace transform is used for frequency dependent storage modulus, loss factor of such NC materials.

Result showed a significant increase in the storage modulus and damping of NC material when the higher volume fraction of MWCNT is mixed in matrix phase, Sravanos-Chamis micromechanics (SCM) and strength of materials (SOM) mathematical models are used to depict the properties of hybrid material system consisting of carbon fiber reinforced PMNC. A MATLAB code is generated to obtain the longitudinal and transverse properties of such materials by increasing the volume fraction of the carbon fiber. Predicted material properties showed that the stiffness and damping are increased significantly by increasing the volume fraction of the carbon fiber in such hybrid material

system. Loss factor and shear loss factor are decreased as the temperature is increases. Several samples of hybrid composite are fabricated consisting of 8% volume fraction of MWCNT in matrix phase and different volume fraction of carbon fiber as reinforcement. Experimental validation is done for such hybrid composites for SCM and SOM methods based numerical results. Longitudinal modulus, transverse modulus and loss factor are depicted in frequency domain. It is cleared from the results that the overall material properties were increased by the inclusion of MWCNTs in the CFRP material system.

Declaration of conflicting interest:

The author(s) declare that there are no potential conflicts of interest with respect to the research, authorship and/or publication of this article.

Acknowledgements

References

Balasubramanian, K. and Burghard, M. (2005), "Chemically functionalized carbon nanotubes", *Small*, **1**(2), 180-192. https://doi.org/10.1002/smll.200400118.

Burgarella, B., Maurel-Pantel, A., Lahellec, N., Bouvard, J.L., Billon, N., Moulinec, H. and Lebon, F. (2018), "Effective viscoelastic behavior of short fibers composites using virtual DMA experiments", *Mech. Time Depend. Mater.*, **23**(3), 337-360. https://doi.org/10.1007/s11043-018-9386-z.

Chandra, R., Singh, S. and Gupta, K. (1999), "Damping studies in fiber-reinforced composites - a review", *Compos. Struct.*, **46**(1), 41-51. https://doi.org/10.1016/s0263-8223(99)00041-0.

Chandra, R., Singh, S.P. and Gupta, K. (2002), "Micromechanical damping models for fiber-reinforced composites: a comparative study", *Compos. Part A: Appl. Sci. Manuf.*, **33**(6), 787-796. https://doi.org/10.1016/s1359-835x(02)00019-2.

Dul, S., Fambri, L. and Pegoretti, A. (2018) "Filaments production and fused deposition modelling of ABS/Carbon nanotubes composites", *Nanomater.*, **8**, 49. https://doi.org/10.3390/nano8010049.

Farjpour, A., Ghayesh, M.H. and Forokhi, H. (2018), "A review on the mechanics of nanostructures", *Eng. Science*, **133**, 231-263. https://doi.org/10.1016/j.ijengsci.2018.09.006.

Ghayesh, M.H. (2019), "Asymmetric viscoelastic nonlinear vibrations of imperfect AFG beams", *Appl. Acoust.*, **154**, 121-128. https://doi.org/10.1016/j.apacoust.2019.03.022.

Ghayesh, M.H. (2019), "Mechanics of viscoelastic functionally graded micro-cantilevers", *Mech.-A/Solid.*, **73**, 492-499. https://doi.org/10.1016/j.euromechsol.2018.09.001.

Ghayesh, M.H. and Farjpour, A. (2019), "A review on the mechanics of functionally graded nanoscale and microscale structures", *Eng. Sci.*, **137**, 8-36. https://doi.org/10.1016/j.ijengsci.2018.12.001.

Gholipour, A. and Ghayesh, M.H. (2020), "A coupled nonlinear nonlocal strain gradient theory for functionally graded Timoshenko nano-beams", *Microsyst. Technol.*, **26**, 2053-2066. http://doi.org/10.1007/s00542-020-04757-1.

Gholipour, A. and Ghayesh, M.H. (2020), "Nonlinear coupled mechanics of functionally graded nano-beams", *Eng. Sci.*, **150**, 103221. https://doi.org/10.1016/j.ijengsci.2020.103221.

Gojny, F.H., Wichmann, M.H.G., Köpke, U., Fiedler, B. and Schulte, K. (2004), "Carbon nanotube-reinforced epoxy-composites: enhanced stiffness and fracture toughness at low nanotube content", *Compos. Sci. Technol.*, **64**(15), 2363-2371. https://doi.org/10.1016/j.compscitech.2004.04.002.

Hirsch, A. (2002), "Functionalization of single-walled carbon manotubes", *Angewandte Chemie Int. Ed.*, **41**(11), 1853. https://doi.org/10.1002/1521-3773(20020603)41.

Iijima, S. (1991), "Helical microtubules of graphitic carbon", *Nature*, **354**(6348), 56-58. https://doi.org/10.1038/354056a0.

Jia, Y., Peng, K., Gong, X. and Zhang, Z. (2011), "Creep and recovery of polypropylene/carbon nanotube composites" *Int. J. Plast.*, **27**(8), 1239-1251. https://doi.org/10.1016/j.ijplas.2011.02.004.

Khan, S.U., Li, C.Y., Siddiqui, N.A. and Kim, J.K. (2011), "Vibration damping characteristics of carbon fiber-reinforced composites containing multi-walled carbon nanotubes", *Compos. Sci. Technol.*, **71**(12), 1486-1494. https://doi.org/10.1016/j.compscitech.2011.03.022.

Knapp, G., Oreski, G. and Pinter, G. (2015), "Method to characterize the damping behavior of thin passively constrained layer laminates using dynamic mechanical analysis (DMA) in shear mode", *Polym. Test.*, **42**, 215-224. https://doi.org/10.1016/j.polymertesting.2015.01.011.

Koratkar, N., Wei, B. and Ajayan, P.M. (2002), "Carbon nanotube films for damping applications", *Adv. Mater.*, **14**(13-14), 997-1000. https://doi.org/10.1002/1521-4095(20020705)14.

Koratkar, N.A., Suhr, J., Joshi, A., Kane, R.S., Schadler, L.S., Ajayan, P.M. and Bartolucci, S. (2005), "Characterizing energy dissipation in singlewalled carbon nanotube polycarbonate composites", *J. Acoust. Soc. Am.*, **126**(4), 2281-2281. https://doi.org/10.1063/1.2007867.

Lin, R.M. and Lu, C. (2010), "Modeling of interfacial friction damping of carbon nanotube-based nanocomposites", *Mech. Syst. Signal Pr.*, **24**(8), 2996-3012. https://doi.org/10.1016/j.ymssp.2010.06.003.

Ma, P.C., Siddiqui, N.A., Marom, G. and Kim, J.K. (2010), "Dispersion and functionalization of carbon nanotubes for polymer-based nanocomposites: A review", *Compos. Part A: Appl. Sci. Manuf.*, **41**(10), 1345-1367. https://doi.org/10.1016/j.compositesa.2010.07.003.

Montazeri, A. and Montazeri, N. (2011), "Viscoelastic and mechanical properties of multi walled carbon nanotube/epoxy composites with different nanotube content", *Mater. Des.*, **32**(4), 2301-2307. https://doi.org/10.1016/j.matdes.2010.11.003.

Rahmanian, S., Suraya, A.R., Shazed, M.A., Zahari, R. and Zainudin, E.S. (2014), "Mechanical characterization of epoxy composite with multiscale reinforcements: Carbon nanotubes and short carbon fibers", *Mater. Des.*, **60**, 34-40. https://doi.org/10.1016/j.matdes.2014.03.039.

Rajoria, H. and Jalili, N. (2005), "Passive vibration damping enhancement using carbon nanotube-epoxy reinforced composites", *Compos. Sci. Technol.*, **65**(14), 2079-2093. https://doi.org/10.1016/j.compscitech.2005.05.015.

Swain, A. and Roy, T. (2017), "Viscoelastic modeling and vibration damping characteristics of hybrid CNTs-CFRP composite shell structures", *Acta Mechanica*, **229**(3), 1321-1352. https://doi.org/10.1007/s00707-017-2051-9.

Swain, A., Baad, S. and Roy, T. (2016), "Modeling and analyses of thermo-elastic properties of radially grown carbon nanotubes-based woven fabric hybrid composite materials", *Mech. Adv. Mater. Struct.*, **24**(14), 1206-1220. https://doi.org/10.1080/15376494.2016.1227498.

Swain, A., Roy, T. and Nanda, B.K. (2016), "Vibration damping characteristics of carbon nanotubes-based thin hybrid composite spherical shell structures", *Mech. Adv. Mater. Struct.*, **24**(2), 95-113. https://doi.org/10.1080/15376494.2015.1107669.

Tehrani, M., Safdari, M. and Al-Haik, M.S. (2011), "Nanocharacterization of creep behavior of multiwall carbon nanotubes/epoxy nanocomposite", *Int. J. Plast.*, **27**(6), 887-901. https://doi.org/10.1016/j.ijplas.2010.10.005.

Theodore, M., Hosur, M., Thomas, J. and Jeelani, S. (2011), "Influence of functionalization on properties of MWCNT-epoxy nanocomposites", *Mater. Sci. Eng. A*, **528**(3), 1192-1200. https://doi.org/10.1016/j.msea.2010.09.095.

Thostenson, E.T. and Chou, T.W. (2006), "Processing-structure-multi-functional property relationship in carbon nanotube/epoxy composites", *Carbon*, **44**(14), 3022-3029. https://doi.org/10.1016/j.carbon.2006.05.014.

Treviso, A., Van Genechten, B., Mundo, D. and Tournour, M. (2015), "Damping in composite materials: Properties and models", *Composites Part B: Engineering*, **78**, 144-152. https://doi.org/10.1016/j.compositesb.2015.03.081.

Yao, Z., Wu, D., Chen, C. and Zhang, M. (2013), "Creep behavior of polyurethane nanocomposites with carbon nanotubes", *Compos. Part A: Appl. Sci. Manuf.*, **50**, 65-72. https://doi.org/10.1016/j.compositesa.2013.03.015.

Zhang, H., Bilotti, E., Tu, W., Lew, C.Y. and Peijs, T. (2015), "Static and dynamic percolation of phenoxy/carbon nanotube nanocomposites", *Eur. Polym. J.*, **68**, 128-138. https://doi.org/10.1016/j.eurpolymj.2015.04.022.

Zhou, X., Shin, E., Wang, K.W. and Bakis, C.E. (2004), "Interfacial damping characteristics of carbon nanotube-based composites", *Compos. Sci. Technol.*, **64**(15), 2425-2437. https://doi.org/10.1016/j.compscitech.2004.06.001.

CC

Appendix

All matrices used for the present study (Swain *et al.* 2016; Swain *et al.*. 2016) are presented below

$$
[C_1] = v_f
\begin{bmatrix}
C_{11}^f & C_{12}^f & C_{12}^f & 0 & 0 & 0 \\
0 & 0 & 0 & 0 & 0 & 0 \\
0 & 0 & 0 & 0 & 0 & 0 \\
0 & 0 & 0 & 0 & 0 & 0 \\
0 & 0 & 0 & 0 & 0 & 0 \\
0 & 0 & 0 & 0 & 0 & 0
\end{bmatrix}
\tag{15}
$$

$$
[C_2] =
\begin{bmatrix}
v_{NC} C_{11}^{NC} & v_{NC} C_{12}^{NC} & v_{NC} C_{12}^{NC} & 0 & 0 & 0 \\
C_{12}^{NC} & C_{11}^{NC} & C_{12}^{NC} & 0 & 0 & 0 \\
C_{12}^{NC} & C_{12}^{NC} & C_{11}^{NC} & 0 & 0 & 0 \\
0 & 0 & 0 & C_{44}^{NC} & 0 & 0 \\
0 & 0 & 0 & 0 & C_{44}^{NC} & 0 \\
0 & 0 & 0 & 0 & 0 & C_{44}^{NC}
\end{bmatrix}
\tag{16}
$$

$$
[C_3] =
\begin{bmatrix}
1 & 0 & 0 & 0 & 0 & 0 \\
C_{12}^f & C_{22}^f & C_{23}^f & 0 & 0 & 0 \\
C_{13}^f & C_{23}^f & C_{22}^f & 0 & 0 & 0 \\
0 & 0 & 0 & C_{44}^f & 0 & 0 \\
0 & 0 & 0 & 0 & C_{55}^f & 0 \\
0 & 0 & 0 & 0 & 0 & C_{55}^f
\end{bmatrix}
\tag{17}
$$

$$
[C_4] =
\begin{bmatrix}
1 & 0 & 0 & 0 & 0 & 0 \\
C_{12}^{NC} & C_{11}^{NC} & C_{12}^{NC} & 0 & 0 & 0 \\
C_{12}^{NC} & C_{12}^{NC} & C_{11}^{NC} & 0 & 0 & 0 \\
0 & 0 & 0 & C_{44}^{NC} & 0 & 0 \\
0 & 0 & 0 & 0 & C_{44}^{NC} & 0 \\
0 & 0 & 0 & 0 & 0 & C_{44}^{NC}
\end{bmatrix}
\tag{18}
$$

$$[V_1] = \begin{bmatrix} 0 & 0 & 0 & 0 & 0 & 0 \\ 0 & v_f & 0 & 0 & 0 & 0 \\ 0 & 0 & v_f & 0 & 0 & 0 \\ 0 & 0 & 0 & v_f & 0 & 0 \\ 0 & 0 & 0 & 0 & v_f & 0 \\ 0 & 0 & 0 & 0 & 0 & v_f \end{bmatrix} \tag{19}$$

$$[V_2] = \begin{bmatrix} 1 & 0 & 0 & 0 & 0 & 0 \\ 0 & v_{NC} & 0 & 0 & 0 & 0 \\ 0 & 0 & v_{NC} & 0 & 0 & 0 \\ 0 & 0 & 0 & v_{NC} & 0 & 0 \\ 0 & 0 & 0 & 0 & v_{NC} & 0 \\ 0 & 0 & 0 & 0 & 0 & v_{NC} \end{bmatrix} \tag{20}$$

$$[V_3] = [V_1] + [V_2][C_4]^{-1}[C_3] \tag{21}$$

$$[V_4] = [V_2] + [V_1][C_3]^{-1}[C_4] \tag{22}$$